Biomaterials Advances 178 (2026) 214459

Contents lists available at ScienceDirect

Biomaterials Advances

journal homepage: www.journals.elsevier.com/materials-science-and-engineering-c

The biocompatibility of a novel polyether ether ketone (PEEK) stoma device with human epidermal keratinocytes

Aaron Palmer [a,b], Racheal Wadlow [b], Anna Chruscik [a,b], Mathilde Maybery [a,c], Paulomi Burey [b,d], Eliza Whiteside [a,b], Nikita Walz [a,b,*]

[a] School of Health and Medical Sciences, University of Southern Queensland, Toowoomba, Queensland, Australia
[b] Centre for Future Materials, University of Southern Queensland, Toowoomba, Queensland, Australia
[c] United Kingdom Health Security Agency (UKHSA), Department of Health and Social Care, London, United Kingdom
[d] School of Agriculture and Environmental Science, University of Southern Queensland, Toowoomba, Queensland, Australia

ARTICLE INFO

Keywords:
Polyether ether ketone
PEEK
Keratinocytes
Biocompatibility
ISO 10993
Medical stoma device
HaCaT cell line
THP-1 cell line

ABSTRACT

Surgical stomas are essential interventions for many medical conditions, however, can create physical complications, such as peristomal skin irritation. Medical stoma devices (MSD) are a potential treatment to mitigate such complications. Polyether ether ketone (PEEK) is a promising material for implantable MSD due to its established biocompatibility within orthodontic and orthopaedic applications. However, its cytocompatibility with human epidermal keratinocytes has not been evaluated according to ISO 10993-5:2009 guidelines. This study aimed to assess the biocompatibility of a novel PEEK MSD with human keratinocytes (HaCaT cells). Cells were cultured on discs of PEEK, surface-modified PEEK (m-PEEK), and polylactic acid (PLA). Surface topography was investigated *via* SEM to assess surface roughness (S_a, S_z), and water contact angle (WCA). m-PEEK demonstrated increased S_a and WCA compared to PLA and unmodified PEEK. Cell proliferation and viability were evaluated using CyQUANT™ and AlamarBlue™ assays and no significant differences were observed among PLA, PEEK, and m-PEEK. Cell adhesion was assessed using an adhesion assay, with m-PEEK demonstrating significantly higher cell adhesion than PLA ($p < 0.05$), with cell attachment confirmed *via* SEM imaging. Cytokine analysis of supernatants using Luminex Immunoassay revealed two (IL-1α and IL-6) of six cytokines outlined in the ISO 10993-20:2006 guidelines were elevated in the presence of PEEK at 72 h. These findings suggest that PEEK is non-cytotoxic and biocompatible with human keratinocytes. Further studies are warranted to assess PEEK's compatibility with colonic cells, 3D skin models, and *in vivo* systems (including for chronic inflammatory responses) for MSD applications.

1. Introduction

Stoma is a surgical procedure that involves exteriorising a portion of the bowel or urinary tract to the anterior abdominal surface [1]. They are implemented for various conditions and diseases, such as bowel or bladder removal, inflammatory bowel disease, colorectal or bladder cancer and diverticulitis [2]. This can pose challenging situations due to the various physiological, physical and psychological complications associated with stomas [3]. One of the major complications (occurring in approximately 70 % of cases) is chronic cutaneous reactions of the peristomal skin [3]. A substantial contributor to this skin irritation is leakage of faecal or urinary matter onto the peristomal skin, and complications associated with continuous and repeated application and removal of adhesive ostomy barriers [4,5]. Despite this, there has been limited development and evaluation of methods to resolve these complications and to improve patient medical and quality of life outcomes.

One promising development in this area is the introduction of artificial medical stoma devices (MSD). Permanent medical devices such as MSD must meet the ISO 10993 guidelines for biocompatibility prior to their application for use in clinical trials supported by regulatory agencies such as the Therapeutic Goods Authority (TGA, Australia), and Food and Drug Administration (FDA, US). One of the most effective MSD to date is the Transcutaneous Implant Evacuation System (TIES® System) developed by OstomyCure, which consists of a transcutaneous mesh-like titanium cylinder [6]. However, metal implants come with several limitations including incompatibility with medical imaging,

* Corresponding author at: School of Health and Medical Sciences, University of Southern Queensland, Toowoomba, Queensland, Australia.
E-mail address: Nikita.Walz@unisq.edu.au (N. Walz).

https://doi.org/10.1016/j.bioadv.2025.214459
Received 12 May 2025; Received in revised form 28 July 2025; Accepted 8 August 2025
Available online 10 August 2025

high thermal conductivity and cytotoxicity from corroded titanium particles overtime [7,8].

Medical grade polymers are a promising alternative to overcome these limitations, such as polyether ether ketone (PEEK). PEEK is a thermoplastic that is currently used as an implantable medical device utilised extensively in commercial orthopaedic and orthodontic applications and has well-established biocompatibility with bone and muscle [9]. Despite PEEK's approval for other biomedical applications, it is not yet been investigated in relation to the skin's biocompatibility. Therefore, the aim of the current study was to characterise a novel MSD made from PEEK and determine whether it meets the ISO 10993 guidelines for biocompatibility with human epidermal keratinocytes.

2. Materials and methods

2.1. Material preparation

The PEEK MSD was designed, manufactured, and supplied by the project sponsor Mr. John Vella (Patent: 2022, Stoma implant assembly, WO 2022/174288 A1, Australia, World Intellectual Property Organisation). The MSD (Fig. 1) was created through injection moulding and consists of both smooth unmodified PEEK (referred throughout as PEEK) surfaces and roughened modified PEEK (m-PEEK) surfaces. To smooth several surfaces of the device photochemical etching was first applied following by electrical discharge machining to create a further roughened surface to the devices modified region. Experimentation was performed on both PEEK and m-PEEK. To isolate sections for experimentation, 5 mm discs were hole-punched using a 5 mm Wad Punch (Boker, NSW, Australia). Untreated 96 well flat bottom polystyrene tissue culture plates (Nunclon Delta, Thermo Fisher, Australia) and polylactic acid (PLA) discs were used as negative controls for cytotoxicity as PLA has established biocompatibility with HaCaT (human skin keratinocyte) cells. PLA (Bambu Lab, Australia) discs were 3D printed *via* fused deposition modelling into a 5 mm (diameter) and 1 mm (height) disc using a X1-Carbon 3D Printer (Bambu Lab, Australia; Supplementary Fig. 1). Sterilisation was achieved by autoclaving the discs at 121 °C for 20 min.

2.2. Material surface analysis

The chemical compositions of the experimental PEEK & m-PEEK were evaluated *via* Fourier Transform Infrared Spectroscopy (FTIR) using a Nicolet iS50 FTIR spectrometer (Thermo Fisher Scientific, WI, US). All spectra were measured from 400 to 4000 cm^{-1} and background spectrum was eliminated from each measurement. Surface analysis was performed using a JCM6000 Scanning Electron Microscope (JEOL Ltd., Japan) to determine the microstructures of PLA, PEEK, and m-PEEK. Discs were attached to conductive carbon tabs then sputter coated with gold nanoparticles using a JEOL Smart Coater (DII-29010SCTR / DII-29030SCTR) before imaging at 100× and 500× magnification. Surface roughness was measured using a digital microscope (Olympus DSX1000) by capturing 3D images at 1080× magnification. Images were analysed using the associated PRECiV™ DSX Software (Olympus, Australia). Arithmetical mean height (S_a) and the maximum height (S_z) were recorded to analyse surface topography. To determine hydrophilicity, water contact angle (WCA) was measured using a digital microscope (Olympus DSX1000). In a temperature-controlled room (22–24 °C), 1 μL of distilled water was pipetted onto the surface of the material. Images were taken after 10 s and processed in ImageJ software to determine the WCA. For all materials tested, surface roughness and WCA measurements were recorded in triplicate, at three different timepoints.

2.3. In vitro keratinocyte cell culture

Human immortalised keratinocyte (HaCaT) and monocyte (THP-1) cell lines were purchased from Thermo Fisher. HaCaT cells were cultured in high glucose Dulbecco's Modified Eagle Medium (DMEM; Merck, Australia) supplemented with 10 % Foetal Bovine Serum (FBS; Merck, Australia). THP-1 cells were cultured in RPMI-1640 Medium (Thermo Fisher, Australia) supplemented with 10 % Foetal Bovine Serum (FBS; Merck, Australia). Cells were maintained at 37 °C in a humidified atmosphere of 5 % CO_2 and 95 % air. THP-1 cells were differentiated into macrophage-like cells by incubation for 48 h with 100 nM phorbol 12-myristate 13-acetate (PMA; Merck, Australia) followed by a 72 h recovery with fresh RPMI-1640 Medium.

2.4. Cell proliferation and viability

Cell proliferation and viability was measured using AlamarBlue™ and CyQUANT™ assays following manufacturers guidelines (Thermo Fisher, Australia). For each protocol, HaCaT cells were cultured separately onto PLA, PEEK, and m-PEEK discs for 24 and 72 h in 96-well plates at a seeding density of 1×10^4 cells/well in 200 μL of DMEM media supplemented with +10 % FBS. Cells were also cultured in polystyrene wells at each time point as a secondary negative control for cytotoxicity as per the ISO 10993-5 guidelines. As a positive control for cytotoxicity, cell death was induced by heating 1×10^4 HaCaT cells at 60 °C for 20 min. To quantify cell numbers, a standard curve was generated by seeding a serial dilution of cells (ranging from 8×10^4 cells/well to 0 cells/well) 18 h prior to performing the assays.

For the CyQUANT™ assay, all media was removed from wells ($n = 6$)

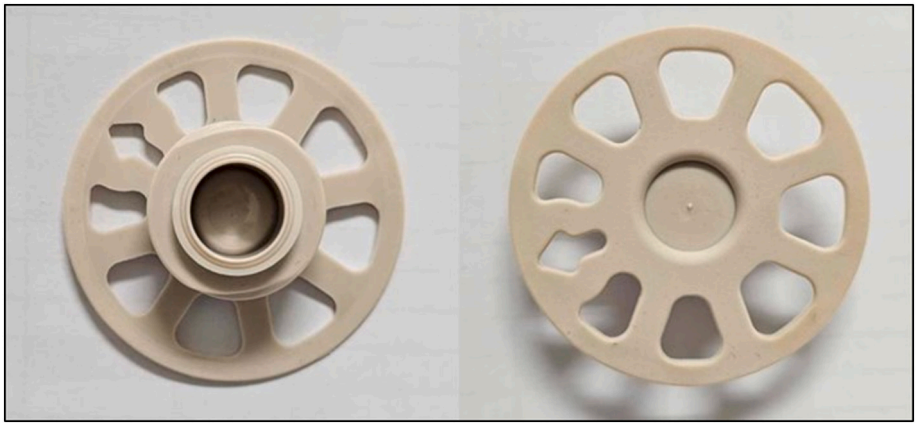

Fig. 1. PEEK implant prototype manufactured *via* injection moulding. The left image displays the smooth-surfaced variant (unmodified PEEK), while the right panel shows the roughened surface modification (modified PEEK). The central circular region in both variants represents the area which is the intended location of the stoma opening.

containing live adherent cells. Positive controls containing suspended dead cells were centrifuged at 300 rpm for 5 min. The supernatant was then removed, and all cells were frozen at −80 °C for 24 h. After 24 h, cells were thawed and resuspended in the CyQUANT® GR dye/cell-lysis buffer reagent and incubated for 5 min at room temperature. Samples were analysed using Varioskan LUX Multimode microplate reader (Thermo Fisher, Australia) with an excitation wavelength of 480 nm and an emission wavelength of 520 nm. The fluorescence was adjusted against blank wells, and the number of cells was calculated based on the standard curve. The cell number was then normalised against the 24 h polystyrene cell counts according to the below formula:

$$\text{Normalised Cell Number}\,(\%) = \frac{\text{Cell Count}}{\text{Cell Count for 24 hour Polystyrene}} \times 100$$

For the AlamarBlue™ assay, 20 μL of AlamarBlue™ solution was added to wells ($n = 3$) and incubated for four hours at 37 °C in a humidified incubator with 5 % CO2. 100 μL of each sample was transferred to a 96 well plate and was analysed for fluorescence intensity using a Varioskan LUX Multimode microplate reader (Thermo Fisher, Australia) with an excitation wavelength of 570 nm and an emission wavelength of 610 nm. The fluorescence was adjusted against blank wells, and the cell number was determined using the standard curve. The cell number was again normalised again the 24 h polystyrene data as previously described.

2.5. Cell morphology analysis

HaCaT cells were cultured on discs for 24 and 72 h in 96-well plates at a seeding density of 1×10^4 cells/well in 200 μL of DMEM media supplemented with 10 % FBS. Following incubation, the media was removed, and the cells were fixed with 2.5 % glutaraldehyde (Merck, Australia) for 24 h at 4 °C. The fixing solution was removed, cells were washed three times in PBS and dehydrated with an ethanol dilution series in PBS (50 %, 70 %, 80 %, 95 % and 100 %) for 10 min per wash at room temperature. Dehydrated samples were then chemically dried using 50 % Bis(trimethylsilyl)amine (HMDS solution; Merck, Australia) for 10 min at room temperature, following replacement with 100 % HMDS solution and allowed for complete evaporation. Samples were then processed for scanning electron microscopy as previously described in section 2.2.

2.6. Adhesion assay

The adhesion assay was based on a previously established protocol although with some modifications [10]. HaCaT cells were cultured on PEEK, m-PEEK and PLA discs ($n = 5$) for 72 h in 96-well plates at a seeding density of 1×10^4 cells/well in 200 μL of DMEM media. After incubation, cells were placed on an IKA® KS 4000i control (IKA, Australia) plate shaker at 320 rpm and 37 °C for 15 min. The media was collected, and cell counts were performed using a TC20 Automated Cell Counter (Biorad, CA, US) to determine the number of detached cells ($N_{Detached}$). Next, 200 μL of TrypLE™ Express Enzyme 1× solution (Merck, Australia) was added to wells which were then shaken at 500 rpm and 37 °C for 10 min to remove remaining cells. The number of cells adhered after the initial shake ($N_{Adherent}$) was counted. The percentage of cells still adhered after the initial 320 rpm shake was calculated using the following formula:

$$\text{Adherent Cells}\,(\%) = \frac{N_{Adherent}}{N_{Adherent} + N_{Detached}} \times 100$$

2.7. Luminex cytokine panel

HaCaT, THP-1 and macrophage cells alone and macrophages and HaCaT cells in co-culture were cultured in the presence and absence of m-PEEK for 72 h. Cytokines were quantified from cell supernatant using the ProcartaPlex™ Human Cytokine Panel 1B, 25plex assay (Thermo Fisher, Australia) using the standard manufacturer's protocol. Briefly, 100 μL of cell culture supernatant was incubated with simplex beads at 600 rpm for 120 min at room temperature. Beads were washed twice with wash buffer and 25 μL of Biotinylated Detection Antibody Mix was added per well and incubated at 600 rpm for 30 min at room temperature. Beads were washed as above then 50 μL of Streptavidin-PE (SA-PE) solution was added per well and incubated at 600 rpm for 30 min at room temperature. Beads were washed (as above), and the plate was shaken at 600 rpm for 5 min at room temperature prior to reading on the Luminex™ 200 instrument (Luminex Corporation, US).

2.8. Statistical analysis

All values are represented as the mean ± standard error of the mean (SEM). Statistical analysis and graph generation was performed using GraphPad Prism version 10 software (La Jolla, CA, US). Statistical significance testing was performed to compare the surface roughness, WCA, normalised cell number, and adhesion strength between PLA, PEEK, m-PEEK, and polystyrene. As per ISO 10993-5 guidelines, a nonsignificant difference ($p > 0.05$) between PEEK materials and PLA (known non-toxic control) would be deemed an indicator of biocompatibility [11]. Statistical significance testing was analysed using ANOVA tests with Tukey post-hoc tests and significance was defined as a p-value <0.05. Graphs were generated using GraphPad Prism 10 software (La Jolla, CA, US).

3. Results

3.1. Surface topography & characterisation

FTIR spectra of the unmodified PEEK & m-PEEK were analysed to determine the chemical composition of the PEEK & m-PEEK surface. FTIR results of both PEEK samples are displayed in Fig. 2 in the form of absorbance as a function of wavenumber (cm^{-1}). Three main absorbance peaks were identified in the 400-650 cm^{-1} region indicating there may be aromatic ring bending or deformation in both PEEK & m-PEEK (Fig. 2). An ether group was identified around 1100 cm^{-1} which may also be indicative of potential ether or aromatic skeletal vibrations. An additional peak at 1200 cm^{-1} was noted in both PEEK samples which suggests C–O–C symmetric stretching. An additional small peak was observed at approximately 1600 cm^{-1}, possibly depicting aromatic C═C stretching. A small peak in the region of 1700 cm^{-1} may be related to the presence of a ketone ring (C═O). Around 3100 cm^{-1}, a single peak was

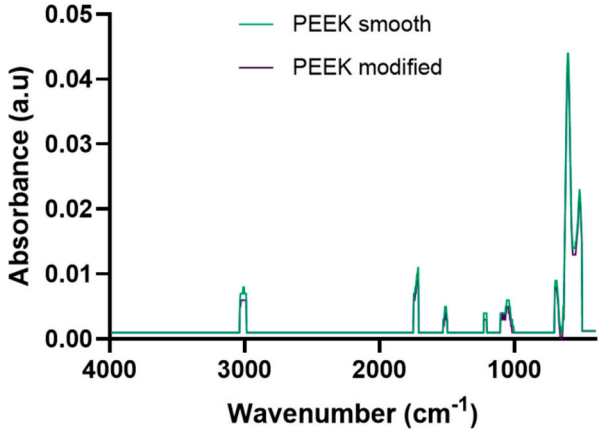

Fig. 2. Fourier transmission infrared (FTIR) spectra of PEEK MSD. Unmodified (smooth PEEK) and modified PEEK surfaces were assessed by FTIR. Data represented with absorbance (arbitrary units) as a function of wavenumber (cm^{-1}).

noted possibly due to C—H stretch vibrations.

The microstructures for PLA, PEEK and m-PEEK are shown in the scanning electron microscopy images below (Fig. 3). The PLA samples (Fig. 3A-B) have relatively flat topography with irregularly spaced divots relative to the unmodified PEEK surface (Fig. 3C-D). These divots were roughly aligned in orientation but varied in size. In comparison, the unmodified PEEK had mild streaking with irregular shallow indentations (Fig. 3C-D). The topography of m-PEEK was considerably rougher (Fig. 3E-F) than either PEEK or PLA. This roughness was irregular with prominent ridges and valleys that appear to vary in size. Within these larger regions, there is additional microtextural variations. However, m-PEEK did not have organised patterns such as regular microgrooves, pores, fibres, or pillars.

Arithmetical mean height (S_a) values for PLA, PEEK and m-PEEK were 3.304 ± 0.245 mm, 3.248 ± 0.098 mm and 4.323 ± 0.327 mm, respectively (Fig. 4A). This indicated that m-PEEK had significantly rougher surface compared to both PEEK and PLA ($p < 0.05$ for both comparisons). This correlates with a significantly higher maximum height (S_z) observed in m-PEEK (38.00 ± 2.868 mm) when compared to both PEEK (20.71 ± 0.7954 mm; $p < 0.0001$) and PLA (4.26 ± 1.860 mm; $p = 0.0002$; Fig. 4B). No significant difference between PEEK and PLA was observed for either S_a or S_z.

Water contact angle (WCA) assay identified that m-PEEK had a significantly higher WCA (72.90 ± 2.875°) compared to PEEK (57.81 ± 1.533°; p = 0.0002) or PLA (57.30 ± 2.082°; $p = 0.0001$) (Fig. 5). There was no significant difference between the WCA of PEEK and PLA.

3.2. Cell proliferation and viability

The results from the CyQUANT™ and AlamarBlue™ assays are shown in Fig. 6. For both assays, cell numbers at each time point showed no significant differences among PLA, PEEK, and m-PEEK surfaces. Additionally, all materials showed a significant increased cell number after 72 h indicating cell proliferation. The CyQUANT™ assay (Fig. 6A) indicated greater cell number in polystyrene wells compared to PLA after 24 h ($p = 0.0115$) and 72 h ($p < 0.01$), and significantly higher cell number in both PEEK and m-PEEK after 72 h ($p < 0.01$ for both). This was not observed in AlamarBlue™ assay (Fig. 6B), which showed no

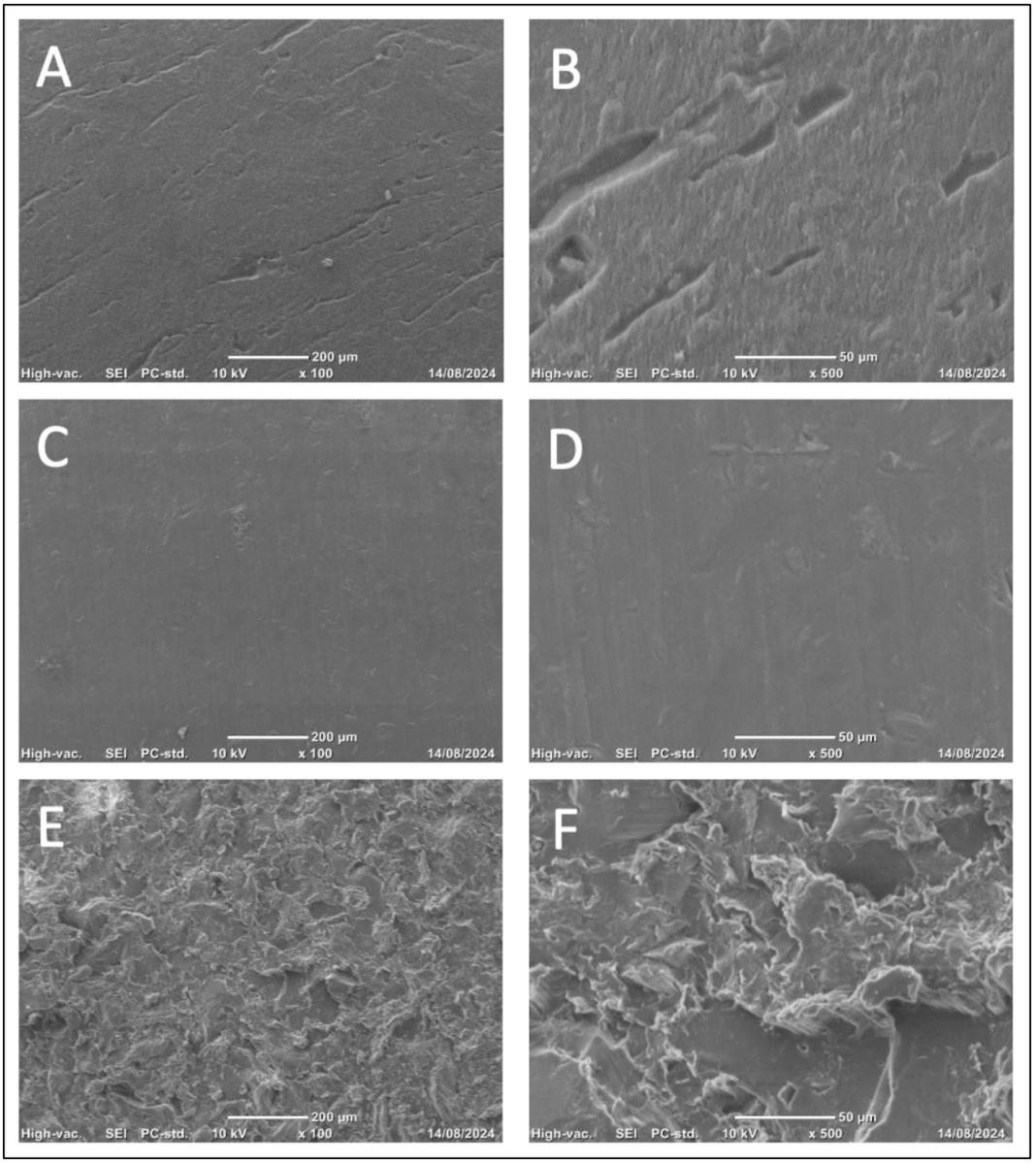

Fig. 3. Scanning electron microscopy images of the surface topography of PLA (A-B), PEEK (C—D) and m-PEEK (E-F). Images were taken at 100× magnification **(A, C, E)** and 500× magnification **(B, D, F).** *Abbreviations: Polylactic acid, PLA; Polyether ether ketone, PEEK; Modified polyether ether ketone, m-PEEK.*

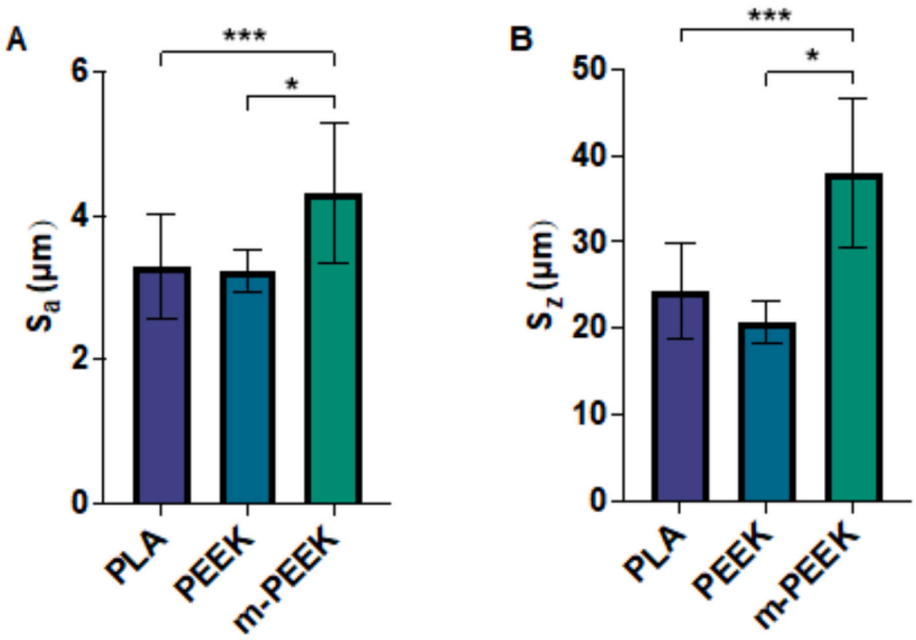

Fig. 4. Surface roughness of PLA, PEEK, and m-PEEK. The surface roughness metrics **(A)** S_a and **(B)** S_z were assessed on PLA, PEEK, and m-PEEK material. Values are represented as the mean ± SEM. * = $p < 0.05$, *** = $p < 0.001$. *Abbreviations: Polylactic acid, PLA; Polyether ether ketone, PEEK; Modified polyether ether ketone, m-PEEK; Arithmetical mean height, S_a; The maximum height, S_z.*

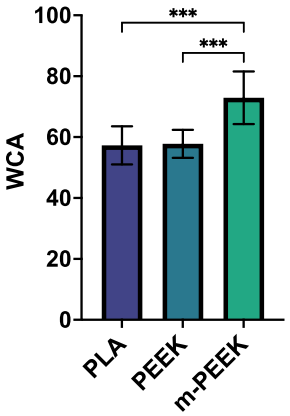

Fig. 5. Water contact angle for PLA, PEEK, and m-PEEK. WCA (°) was assessed at ambient temperature on PLA, PEEK, and m-PEEK materials. Values are represented as the mean ± SEM. *** = $p < 0.001$. *Abbreviations: Polylactic acid, PLA; Polyether ether ketone, PEEK; Modified polyether ether ketone, m-PEEK; Water Contact Angle, WCA.*

differences in cell number between polystyrene and any other material. CyQUANT™ assay reagent stains the DNA of cells (alive or dead), normalising the positive control cell number to 69.642 ± 7.767 %. The AlamarBlue™ assay requires living cells to metabolise the reagent, indicating the normalised cell number for the positive control as 0.994 ± 0.673 %.

3.3. Cell morphology analysis

Scanning electron microscopy images (Fig. 7) revealed distinct morphological characteristics of HaCaT cells cultured on PLA, PEEK, and m-PEEK surfaces. Both PEEK and m-PEEK displayed cell morphological changes from 24 h (Fig. 7C and E) to 72 h (Fig. 7D and F). This change is from singular spheroid-shaped cells at 24 h to a cellular monolayer consisting of flattened and well-spread cell shapes at 72 h. Spheroid cells had an average diameter of 12 µm, while flattened cells measured between 20 µm and 30 µm in diameter. These cell sizes were consistent across all materials. Additionally, HaCaT cells cultured on PEEK and m-PEEK surfaces displayed clear cytoplasmic extensions, such as filopodia, connecting cells to create cell unions at the timepoint. This morphological shift was not observed on cells cultured on PLA surface, which retained the spheroidal structure at the 72 h timepoint (Fig. 7B). Furthermore, the autoclaving and dehydration process appeared to degrade the PLA, as evident by small fragments shown in Fig. 7A-B, which also appeared to have adhered to cells on the surface.

3.4. Cell adhesion

Cell adhesion results indicate that after the initial 320 rpm shake, m-PEEK had the highest percentage of cell adhesion (40.86 ± 5.718 %), followed by PEEK (28.68 ± 6.562 %) (Fig. 8). HaCaT cells cultured on PLA surface displayed lowest cell adhesion (17.22 ± 2.499 %), which was significantly reduced when compared to m-PEEK ($p = 0.0232$, Fig. 8). However, no statistical significance was observed between PEEK, PLA, & m-PEEK.

3.5. Cytokine profile and immune response

The ProcartaPlex™ Human Cytokine Panel 1B (Thermo Fisher, Australia) assays 25 different protein targets, listed in Supplementary Table 1. Six cytokines (interferon gamma, IFN-γ; interleukin-1 alpha, IL-1α; interleukin-6, IL-6; interleukin-10, IL-10; tumour necrosis factor alpha, TNF-α; and tumour necrosis factor beta, TNF-β) highlighted by the 10,993–20:2006 guidelines (Principles and methods for immunotoxicology testing of medical devices [12]) are reported here. Results of the the full cytokine panel are detailed in Supplementary Fig. 4 & Table 1. The expression of two cytokines IL-1α and IL-6, was significantly increased in cells co-cultured with PEEK, compared to those co-cultured without PEEK ($p < 0.0001$, Fig. 9). There was no significant change in the remaining four cytokines (IFNγ, IL-10, TNF-α, and TNF-β).

4. Discussion

This study demonstrated that both the unmodified and modified

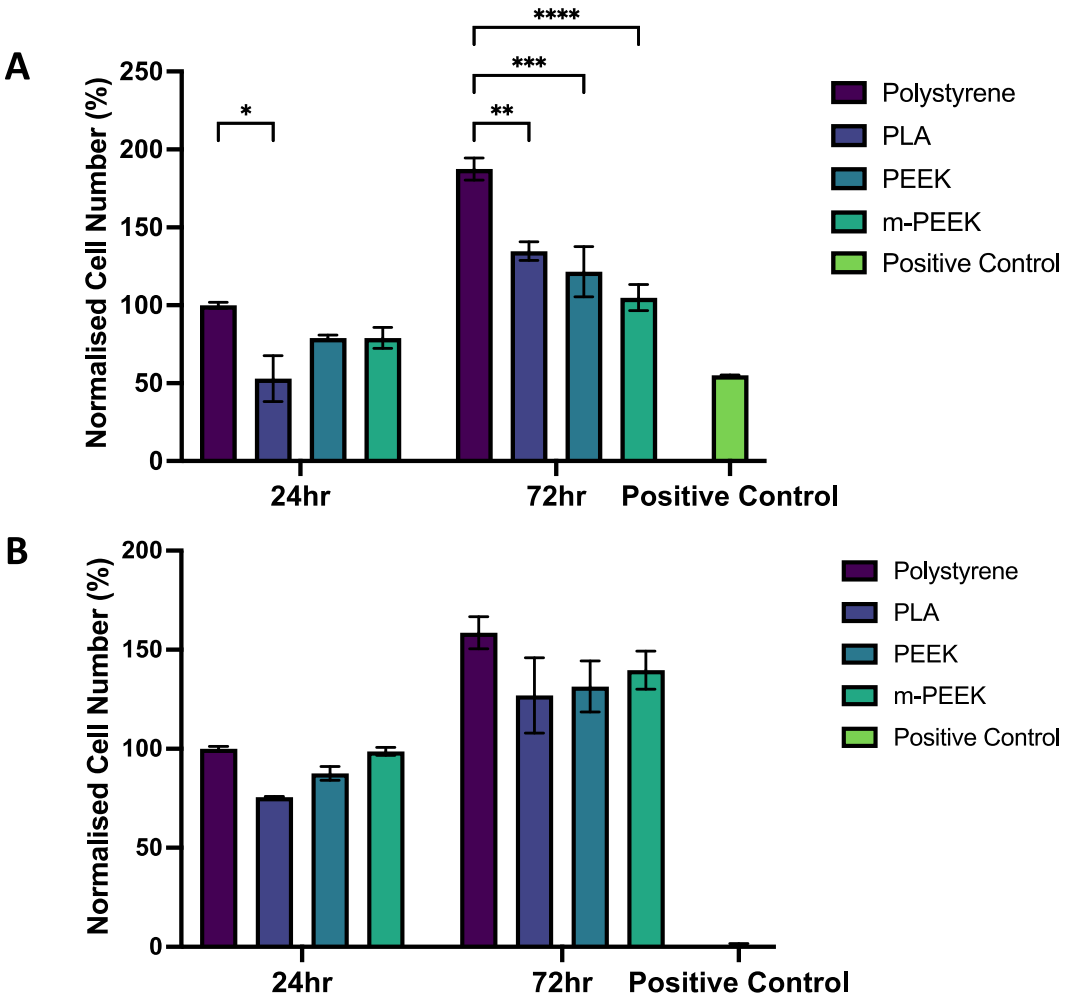

Fig. 6. Comparison of HaCaT cell viability with polystyrene, PLA, PEEK, and m-PEEK after 24 and 72 h. Assessment of cell viability in HaCaT cells using **A)** CyQUANT™ and **B)** AlamarBlue™ assay in the presence of polystyrene cell culture wells, PLA, PEEK, and m-PEEK. The positive control for cytotoxicity contains 1×10^4 dead HaCaT cells. Values are represented as the mean ± SEM. * = $p < 0.05$, ** = $p < 0.01$, *** = $p < 0.001$, **** = $p < 0.0001$. *Abbreviations: Polylactic acid, PLA; Polyether ether ketone, PEEK; Modified polyether ether ketone, m-PEEK.*

PEEK are biocompatible with human epidermal keratinocytes according to the ISO 10993-5 guidelines for *in vitro* cytotoxicity [11]. The other major findings from the characterisation analyses were that:

1. m-PEEK had a significantly higher surface roughness and higher WCA than both PEEK and PLA, while no significant differences in surface characteristics between PEEK and PLA were observed.
2. m-PEEK had superior cell adhesion properties and induced greater changes in cell morphology compared to PEEK and PLA.
3. Immunological results showed two of the six cytokines outlined in the ISO 10993-20:2006 guidelines [12] were significantly increased in the conditioned media of cells cultures in the presence of PEEK compared to cells without PEEK (one pro-inflammatory and one multifunctional cytokine).

The spectra for both samples displayed comparable peak positions across the measured range, indicating that the core chemical structure of PEEK is preserved following surface modification. The results here are in line with literature assessing unmodified PEEK for surface chemical composition as determined by FTIR with a similar core structure shown [13]. Characteristic peaks associated with aromatic C═C stretching (1600 cm^{-1}), ether linkages (asymmetric and symmetric C–O–C stretching around 1300–1200 cm^{-1}), and aromatic skeletal vibrations (1100 cm^{-1}) were observed in both spectra, confirming the presence of the expected functional groups in the polyether ether ketone backbone. Despite the overall spectral similarity, subtle differences were noted. Specifically, the PEEK modified sample exhibited a slight reduction in peak intensity within the 1200–1000 cm^{-1} region. This decrease may be attributed to partial surface oxidation or chemical restructuring resulting from the photochemical etching process. These modifications are likely to enhance surface reactivity or hydrophilicity while maintaining the desirable mechanical and chemical stability of the base material. Further studies using surface-sensitive techniques such as X-ray Photoelectron Spectroscopy (XPS) are recommended to confirm and quantify more specific chemical changes induced by photochemical modification of PEEK and the biological significance of such changes.

Surface topography is a critical determinant of cell adhesion and growth. In this study, m-PEEK exhibited significantly greater surface roughness compared to both unmodified PEEK and PLA, providing increased adhesion points that are known to enhance cell proliferation [14]. However, the influence of surface topography is also dependent on the degree of roughness and the presence of microfeatures such as microgrooves or pillars, which can direct cell orientation and differentiation [15]. The surface of m-PEEK was irregular but lacked defined microfeatures. To control for the effects of surface roughness, PLA discs were 3D printed to achieve a comparable surface roughness [16]. Surface roughness measurements confirmed no significant difference between PLA and PEEK, ensuring that observed differences in cellular

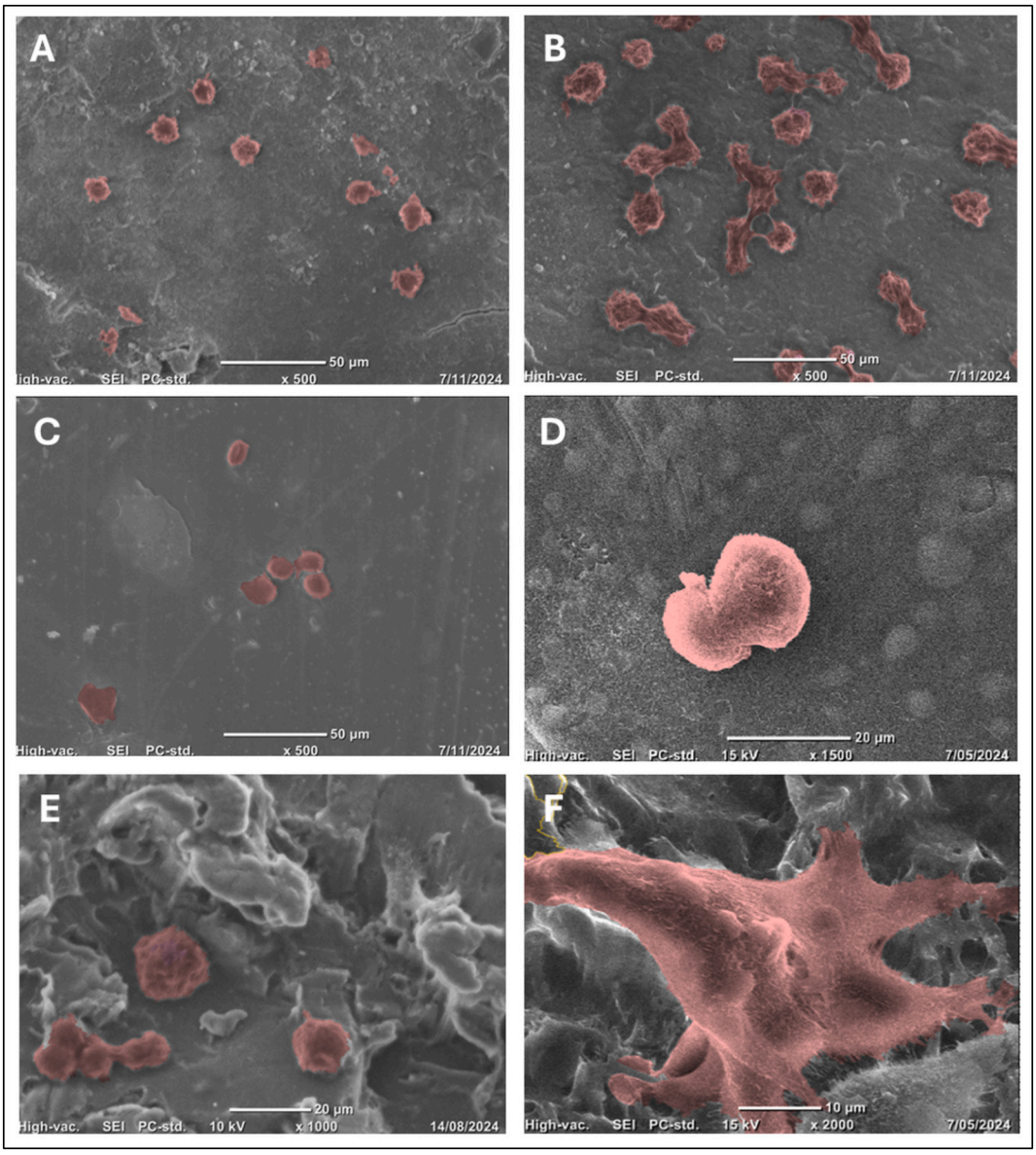

Fig. 7. SEM images of HaCaT cells cultured on PLA (A-B), PEEK (C—D), and m-PEEK (*E*-F). Cells were incubated for 24 h **(A, C, E)** and 72 h **(B, D, F)**. Pseudo colouring was applied in MountainsLab® software (Digital Surf, Switzerland) to enhance contrast and aid visual interpretation of SEM images. Images displayed are between 500-2000× magnification. *Abbreviations: Polylactic acid, PLA; Polyether ether ketone, PEEK; Modified polyether ether ketone, m-PEEK.*

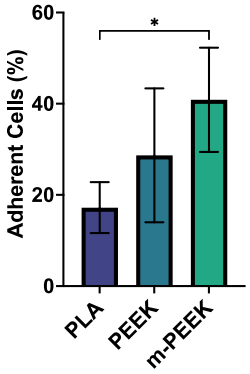

Fig. 8. HaCaT cell adhesion on PLA, PEEK, and m-PEEK after 72 h. Values are represented as the mean ± SEM. * = $p < 0.05$. *Abbreviations: Polylactic acid, PLA; Polyether ether ketone, PEEK; Modified polyether ether ketone, m-PEEK.*

interactions are attributable to material composition rather than topographical variation.

Surface roughness can also affect wettability [17]. The WCAs of PEEK and PLA were similar, consistent with previous reports indicating typical ranges of 70–90° for PEEK and 75–85° for PLA [18,19]. However, the measured WCAs in this study were lower than these ranges; for example, Ma and Guo [20] reported a WCA of 75.6 ± 1.9° for injection-moulded PEEK, compared to 57.81 ± 1.53° observed here. Such discrepancies likely reflect variations in manufacturing methods and measurement protocols [20–22]. WCA data presented here may suggest the roughened surface m-PEEK is creating air pockets which become trapped beneath the liquid droplets during testing, effectively reducing the contact area between the liquid and the solid surface as explained by the Cassie-Baxter equation. Importantly, all materials exhibited WCAs below 90°, suggesting hydrophilicity, which is favourable for protein adsorption and subsequent cell adhesion [23], however chemical composition and surface energy of the device and the implications for protein adsorption requires further evaluation to elucidate the surface characterisation.

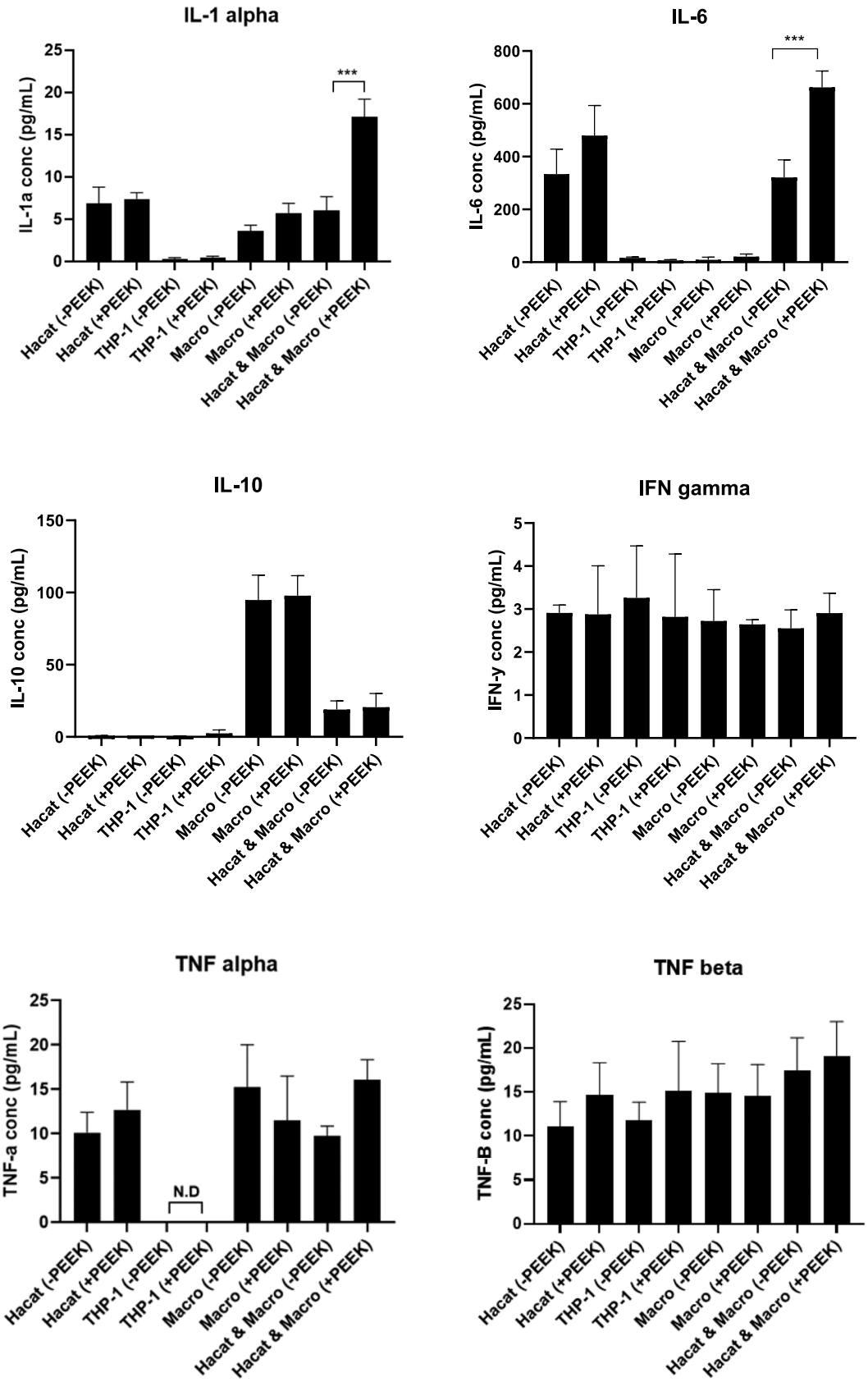

Fig. 9. The immune response of HaCaT, THP-1, and macrophages cultured in the presence and absence of PEEK. HaCaT, THP-1 and macrophage cells were cultured alone for 72 h with (+) and without (−) PEEK. HaCaT cells were also cultured in co-culture with macrophage cells for 72 h with and without PEEK. Cytokines were quantified using the ProcartaPlex™ Human Cytokine Panel 1B, 25plex assay (Thermo Fisher, Australia). *Abbreviations: N·D, not detected; Macro, macrophages.*

Both the CyQUANT™ and AlamarBlue™ assays demonstrated no significant differences in the number of viable HaCaT cells cultured on PLA, PEEK, or m-PEEK. As PLA is a widely accepted non-cytotoxic, biocompatible polymer [24,25], its inclusion as a negative control aligns with ISO 10993-5 guidelines, which recommend comparison against a non-cytotoxic material to assess *in vitro* cytotoxicity [12]. The agreement between both assays reinforces the reliability of these findings. The AlamarBlue™ assay evaluates cell viability based on metabolic activity, indicating that cells on all materials were metabolically active and proliferating [26]. Given that metabolic activity can be influenced by factors such as cellular stress and media conditions, results were corroborated using the CyQUANT™ assay, which more directly quantifies cell number *via* nucleic acid staining [27,28]. Positive controls yielded the expected cytotoxic response in both assays, further validating assay performance in accordance with ISO 10993-5 requirements [11]. Although higher cell numbers were observed on polystyrene wells (CyQUANT™), this was expected due to the Nunclon™ Delta (Thermo Fisher) surface treatment of cell culture plastics that promote optimal cell growth. Notably, AlamarBlue™ results did not show a significant advantage for polystyrene, supporting the conclusion that PEEK, and m-PEEK are not cytotoxic. The lower cell counts observed with the CyQUANT™ assay may reflect cell loss during washing, rather than true differences in viability. Taken together, this data suggests that PEEK supports keratinocyte viability and meets the ISO 10993-5 criteria for *in vitro* biocompatibility.

To date, only two prior studies have reported culturing human epidermal keratinocytes on PEEK [29,30]. However, neither study adhered to ISO 10993-5 guidelines. Saad et al. [30] assessed surface modifications to enhance HaCaT growth on PEEK and titanium but did not include a non-cytotoxic polymer control. Similarly, Ekambaram and Dharmalingam [29] investigated sulphonated PEEK nanofibers as drug carriers, focusing on processing parameters rather than biocompatibility assessment. These studies also lacked appropriate negative and positive controls. Moreover, findings on modified PEEK nanostructures cannot be extrapolated to unmodified solid PEEK discs. To the authors' knowledge, this is the first study to evaluate and confirm the biocompatibility of unmodified PEEK with human epidermal keratinocytes in accordance with ISO 10993-5 guidelines for *in vitro* cytotoxicity, supporting its potential use in long-term medical skin devices (MSDs).

While limited research exists on PEEK's interaction with human epidermal keratinocytes, several studies have investigated its biocompatibility with other soft tissues, such as gingival keratinocytes and gingival fibroblasts [10,22]. Unmodified PEEK generally supports lower proliferation of gingival keratinocytes compared to titanium, and this has been attributed to its relatively flat surface topography, despite titanium exhibited a lower WCA [22,36,37]. Similar findings have been reported for gingival fibroblasts, where cell proliferation on unmodified PEEK was inferior to titanium or zirconia surfaces [10,21,31].

Surface modification of PEEK to increase roughness has been shown to enhance cellular response. m-PEEK demonstrates comparable biocompatibility to titanium and zirconia in both immortalised and primary human-derived gingival keratinocytes, with positive outcomes observed over extended culture periods (1–10 days) [22,32,33]. Likewise, gingival fibroblasts cultured on roughened PEEK surfaces exhibit equal or superior proliferation compared to those on titanium or zirconia [10,22,33–36]. Furthermore, inflammatory cytokine expression (IL-1β, IL-6, TNF-α) by gingival fibroblasts following 24 h exposure to PEEK is comparable to that induced by Ti-6Al-4 *V*, PEKK, and Y-TZP [34]. Collectively, these findings support the conclusion that PEEK is biocompatible with soft tissues, although surface modification may be necessary for cell attachment and proliferation. Despite titanium's superior cell-supporting properties, its clinical use is limited by drawbacks such as incompatibility with medical imaging, high thermal conductivity, and the potential cytotoxicity of corrosion products over time [7,8].

A notable limitation of the present study is the 72 h time frame, whereas the literature demonstrates PEEK's suitability for longer-term soft tissue compatibility [22,33,35].Establishing long-term biocompatibility is critical for applications involving permanent MSD. Encouragingly, PEEK's high chemical and thermal stability reduces the likelihood of altered biocompatibility over time [37], and degradation particles have been shown to elicit minimal cytotoxic or immune responses [38]. The adhesion assay indicated that m-PEEK supported superior HaCaT cell adhesion, likely due to increased cell morphology changes observed after 72 h. Cells on PLA remained spheroid, aligning with previous reports that attribute poor PLA adhesion to a lack of surface functional groups, rendering it bioinert [39,40]. Verification of these findings would require surface chemical analysis, such as X-ray photoelectron spectroscopy. These findings suggest that PEEK and m-PEEK offer improved adhesion properties, which is critical for MSD exposed to shear forces. No previous studies have evaluated PEEK's adhesion to human epidermal keratinocytes; however, studies using gingival fibroblasts reported a non-significant trend toward superior adhesion on PEEK compared to titanium and zirconia [10]. PLA's poor adhesion likely affected the 24 h CyQUANT™ assay results. Similarly, SEM at 72 h showed fewer adherent cells on PLA than on PEEK or m-PEEK, despite comparable cell numbers in the AlamarBlue™ assay. These discrepancies suggest cell detachment during cell washing procedures.

Although m-PEEK had increased roughness compared to PEEK, this did not translate into enhanced cell proliferation. This may be due to increased surface roughness also increasing WCA, thereby reducing hydrophilicity, as reported in prior studies [21]. Similar findings have been observed in gingival keratinocyte models, where increased roughness did not always correlate with improved growth [21]. Nevertheless, m-PEEK showed a non-significant trend toward improved adhesion over PEEK, likely due to roughened surfaces providing more anchorage points for cell attachment [41]. Therefore, m-PEEK may offer advantages *in vivo* under dynamic conditions involving shear stress.

A limitation of this study is the use of an *in vitro* HaCaT monoculture, which does not replicate the complex immune signaling environment of human skin. Keratinocytes play a critical role in initiating inflammation by secreting cytokines (*e.g.*, IL-1, TNF-α), interferons (*e.g.*, IFN-γ), chemokines, and antimicrobial peptides [42,43]. However, *in vitro* monocultures lack immune cells such as monocytes and neutrophils required for activating pro-inflammatory cytokines *via* caspase-1 [44]. In this study, co-cultures of HaCaT cells with macrophages exposed to PEEK showed increased levels of IL-1α and IL-6. IL-1a is a key alarmin released upon cell stress, signaling early tissue irritation or inflammation. IL-6 is a multifunctional cytokine which can be involved in pro- and anti-inflammatory pathways, depending on context. In its pro-inflammatory function, IL-6 can be upregulated for immune cell recruitment and the acute-phase response. In contrast, in its anti-inflammatory function IL-6 can induce other anti-inflammatory cytokines such as IL-10 or inhibit TNF-α (which were both unchanged in the present study) [45]. The elevation of these cytokines in context of one another suggests there may be an acute inflammatory response in cells exposed to PEEK, and although indicative of cell stress, it did not result in a reduction of cell proliferation or viability. The present study corroborates previous findings that co-culture models yield different cytokine profiles and viability outcomes compared to monocultures [46]. Therefore, while monoculture is appropriate for *in vitro* cytotoxicity testing under ISO 10993-5 guidelines, further validation in co-culture and *in vivo* models is essential. Future work should also assess the chronic immune response in accordance with the ISO 10993-20:2006 guidelines for immunotoxicology which can be confirmed with histological evidence of tissue inflammation *in vivo* [47]. Furthermore, in the present study PEEK was used alone to assess cytokine profiles and whilst our data suggests the core chemical composition of the surface of PEEK and m-PEEK are comparable, subtle differences in surface chemistry may be present and could alter the immune profile.

Another important consideration of the study is the use of HaCaT cells, an immortalised human keratinocyte cell line genetically modified

to support continuous proliferation [48,49]. Immortalised cells often exhibit increased resistance to stress and reduced sensitivity to cytotoxic or inflammatory stimuli compared to primary cells, potentially leading to more favourable biocompatibility outcomes [48,49]. As a result, materials deemed non-cytotoxic in immortalised cell models may still elicit adverse responses in primary human keratinocytes. However, studies using gingival keratinocytes have reported comparable results between immortalised and primary cell lines, suggesting that immortalised models can provide relevant insights in certain contexts [22,32]. While the ISO 10993-5 guidelines do not mandate the use of primary cell lines, this factor should be considered when interpreting the present study's findings.

5. Conclusion

This study aimed to characterise a novel MSD made from PEEK to determine whether it meets the ISO 10993 guidelines for biocompatibility with human keratinocytes. The results from this study suggest that PEEK in short-term exposure is biocompatible with human epidermal keratinocytes, meeting the ISO 10993-5 guideline for *in vitro* cytotoxicity, however there are indications of early immune function upregulation. These results are significant because they are an important step forward for the development of an MSD made from PEEK. Furthermore, this opens the door for PEEK to be implemented in other epidermal applications and could even inform decisions regarding superficial medical implants. However, since this is a pre-clinical *in vitro* pilot study, PEEK's biocompatibility would need to be further evaluated through co-cultures and *in vivo* testing. Future studies should also investigate if PEEK is biocompatible with additional stoma-specific cells such as colon cells that the MSD may also interact with and use animal or human models to confirm the findings.

CRediT authorship contribution statement

Aaron Palmer: Writing – review & editing, Writing – original draft, Visualization, Methodology, Investigation, Formal analysis, Data curation. **Racheal Wadlow:** Writing – review & editing, Visualization, Validation, Resources, Methodology, Investigation, Formal analysis. **Anna Chruscik:** Writing – review & editing, Writing – original draft, Supervision, Resources, Project administration, Investigation, Formal analysis, Data curation. **Mathilde Maybery:** Writing – review & editing, Validation, Project administration, Methodology, Investigation, Formal analysis, Conceptualization. **Paulomi Burey:** Writing – review & editing, Validation, Resources, Project administration, Methodology, Investigation, Funding acquisition, Formal analysis, Conceptualization. **Eliza Whiteside:** Writing – review & editing, Writing – original draft, Validation, Supervision, Resources, Project administration, Methodology, Investigation, Funding acquisition, Data curation, Conceptualization. **Nikita Walz:** Writing – review & editing, Writing – original draft, Visualization, Validation, Supervision, Resources, Project administration, Methodology, Investigation, Funding acquisition, Formal analysis, Data curation, Conceptualization.

Declaration of Generative AI and AI-assisted technologies in the writing process

No generative AI tools were used in the creation of this manuscript.

Funding

This work was supported by Mr. John Vella from MACJOL [contract number 23–1382] as part of the Vella-Stoma Research Agreement (29/08/2023).

Declaration of competing interest

The authors declare the following financial interests/personal relationships which may be considered as potential competing interests: Nikita Walz reports financial support was provided by MACJOL Pty Ltd. Nikita Walz reports a relationship with MACJOL Pty Ltd that includes: funding grants. No authors are on the patent has patent #WO 2022/174288 A1 licensed to John Vella. If there are other authors, they declare that they have no known competing financial interests or personal relationships that could have appeared to influence the work reported in this paper.

Acknowledgements

The authors would like to acknowledge Mr. John Vella and the Andresen family for donating the PEEK material for experimentation and funding the project costs. We would like to thank the technical staff at the University of Southern Queensland who helped with training and research support associated with the project.

Appendix A. Supplementary data

Supplementary data to this article can be found online at https://doi.org/10.1016/j.bioadv.2025.214459.

Data availability

Data will be made available on request.

References

[1] B. Hill, Stoma care: procedures, appliances and nursing considerations, Br. J. Nurs. 29 (22) (2020) S14–S19.
[2] E.B. Rivet, Ostomy management: a model of interdisciplinary care, Surg. Clin. North Am. 99 (5) (2019) 885–898.
[3] G. Salvadalena, Incidence of complications of the stoma and peristomal skin among individuals with colostomy, ileostomy, and urostomy: a systematic review, J. Wound Ostomy Continence Nurs. 35 (6) (2008) 596–607.
[4] I. Claessens, R. Probert, C. Teilemans, The ostomy life study: the everyday challenges faced by people living with a stoma in a snapshot, Gastrointest. Nurs. 13 (5) (2015) 18–25.
[5] G. Grove, T. Houser, G. Sibbald, G. Salvadalena, Measuring epidermal effects of ostomy skin barriers, Skin Res. Technol. 25 (2) (2019) 179–186.
[6] K. Strigård, T. Öresland, J. Rutegård, U. Gunnarsson, Transcutaneous implant evacuation system: a new approach to continent stoma construction, Color. Dis. 13 (11) (2011) e379–e382.
[7] S.M. Zol, M.S. Alauddin, Z. Said, M.I. Mohd Ghazali, L. Hao-Ern, D.A. Mohd Farid, N.A.H. Zahari, A.H.A. Al-Khadim, A.H. Abdul Aziz, Description of poly(aryl-etherketone) materials (PAEKs), polyetheretherketone (PEEK) and polyetherketoneketone (PEKK) for application as a dental material: a materials science review, Polymers 15 (9) (2023) 2170.
[8] E. Kandaswamy, M. Harsha, V.M. Joshi, Titanium corrosion products from dental implants and their effect on cells and cytokine release: a review, J. Trace Elem. Med. Biol. 84 (2024) 127464–127464.
[9] N. Enkling, M. Marder, S. Bayer, W. Gotz, M. Stoilov, D. Kraus, Soft tissue response to different abutment materials: a controlled and randomized human study using an experimental model, Clin. Oral Implants Res. 33 (6) (2022) 667–679.
[10] A.S. Rozeik, M.S. Chaar, S. Sindt, S. Wille, C. Selhuber-Unkel, M. Kern, S. El-Kholy, C. Dörfer, K.M.F. El-Sayed, Cellular properties of human gingival fibroblasts on novel and conventional implant-abutment materials, Dent. Mater. 38 (3) (2022) 540–548.
[11] I.O.o. Standardization, Biological evaluation of medical devices, Part 5: Tests for in vitro cytotoxicity, 2009.
[12] I.O.o. Standardization, Biological evaluation of medical devices, Part 20: Principles and methods for immunotoxicology testing of medical devices, 2006.
[13] S. Yasin, A. Shakeel, M. Ahmad, A. Ahmad, T. Iqbal, Physico-chemical analysis of semi-crystalline PEEK in aliphatic and aromatic solvents, Soft Materials 17 (2) (2019) 143–149.
[14] D. Yu, X. Lei, H. Zhu, Modification of polyetheretherketone (PEEK) physical features to improve osteointegration, Journal of Zhejiang University-SCIENCE B 23 (3) (2022) 189–203.
[15] N.O. Monteiro, J.F. Fangueiro, R.L. Reis, N.M. Neves, Replication of natural surface topographies to generate advanced cell culture substrates, Bioactive Materials 28 (2023) 337–347.
[16] S. Stelton, CE: stoma and Peristomal skin care: a clinical review, Am. J. Nurs. 119 (6) (2019) 38–45.

[17] A. Katzer, H. Marquardt, J. Westendorf, J.V. Wening, G. von Foerster, Polyetheretherketone–cytotoxicity and mutagenicity in vitro, Biomaterials 23 (8) (2002) 1749–1759.
[18] W. Wang, C.J. Luo, J. Huang, M. Edirisinghe, PEEK surface modification by fast ambient-temperature sulfonation for bone implant applications, J. R. Soc. Interface 16 (152) (2019) 20180955.
[19] E.H. Tümer, H.Y. Erbil, N. Akdoğan, Wetting of Superhydrophobic Polylactic acid micropillared patterns, Langmuir 38 (32) (2022) 10052–10064.
[20] R. Ma, D. Guo, Evaluating the bioactivity of a hydroxyapatite-incorporated polyetheretherketone biocomposite, J. Orthop. Surg. Res. 14 (1) (2019) 32.
[21] M. Gheisarifar, G.A. Thompson, C. Drago, F. Tabatabaei, M. Rasoulianboroujeni, In vitro study of surface alterations to polyetheretherketone and titanium and their effect upon human gingival fibroblasts, J. Prosthet. Dent. 125 (1) (2021) 155–164.
[22] P. Bagchi, A.A. Alfawzan, S.M. Magar, R. Priya, A.S. Kochhar, S. Agrawal, F. J. AlMutairi, An in vitro evaluation of effect of implant abutment on human gingival epithelial keratinocytes, Ann. Afr. Med. 21 (3) (2022) 217–222.
[23] L. Chen, C. Yan, Z. Zheng, Functional polymer surfaces for controlling cell behaviors, Mater. Today 21 (1) (2018) 38–59.
[24] D. da Silva, M. Kaduri, M. Poley, O. Adir, N. Krinsky, J. Shainsky-Roitman, A. Schroeder, Biocompatibility, biodegradation and excretion of polylactic acid (PLA) in medical implants and theranostic systems, Chem. Eng. J. 340 (2018) 9–14.
[25] F. Diomede, A. Gugliandolo, P. Cardelli, I. Merciaro, V. Ettorre, T. Traini, R. Bedini, D. Scionti, A. Bramanti, A. Nanci, S. Caputi, A. Fontana, E. Mazzon, O. Trubiani, Three-dimensional printed PLA scaffold and human gingival stem cell-derived extracellular vesicles: a new tool for bone defect repair, Stem Cell Res Ther 9 (1) (2018) 104.
[26] F. Bonnier, M.E. Keating, T.P. Wróbel, K. Majzner, M. Baranska, A. Garcia-Munoz, A. Blanco, H.J. Byrne, Cell viability assessment using the Alamar blue assay: a comparison of 2D and 3D cell culture models, Toxicol. in Vitro 29 (1) (2015) 124–131.
[27] L.J. Jones, M. Gray, S.T. Yue, R.P. Haugland, V.L. Singer, Sensitive determination of cell number using the CyQUANT cell proliferation assay, J. Immunol. Methods 254 (1–2) (2001) 85–98.
[28] V.M. Quent, D. Loessner, T. Friis, J.C. Reichert, D.W. Hutmacher, Discrepancies between metabolic activity and DNA content as tool to assess cell proliferation in cancer research, J. Cell. Mol. Med. 14 (4) (2010) 1003–1013.
[29] R. Ekambaram, S. Dharmalingam, Fabrication and evaluation of electrospun biomimetic sulphonated PEEK nanofibrous scaffold for human skin cell proliferation and wound regeneration potential, Mater. Sci. Eng. C 115 (2020) 111150.
[30] A. Saad, C. Penaloza Arias, M. Wang, O. ElKashty, D. Brambilla, F. Tamimi, M. Cerruti, Biomimetic strategy to enhance epithelial cell viability and spreading on PEEK implants, ACS Biomater Sci. Eng. 8 (12) (2022) 5129–5144.
[31] R.C. Cecato, E.F. Martinez, C.A.M. Benfatti, Analysis of the viability and morphology of gingival cells on materials used in novel prosthetic components: in vitro study, J. Contemp. Dent. Pract. 23 (1) (2022) 22–30.
[32] L.L. Ramenzoni, T. Attin, P.R. Schmidlin, In vitro effect of modified polyetheretherketone (PEEK) implant abutments on human gingival epithelial keratinocytes migration and proliferation, Materials (Basel). 12 (9) (2019).
[33] M.A. Osman, E. Kushnerev, R.A. Alamoush, K.G. Seymour, J.M. Yates, Two gingival cell lines response to different dental implant abutment materials: an *in vitro* study, Dent J (Basel) 10 (10) (2022).
[34] T.-Y. Peng, Y.-H. Shih, S.-M. Hsia, T.-H. Wang, P.-J. Li, D.-J. Lin, K.-T. Sun, K.-C. Chiu, T.-M. Shieh, In vitro assessment of the cell metabolic activity, cytotoxicity, cell attachment, and inflammatory reaction of human oral fibroblasts on polyetheretherketone (PEEK) implant–abutment, Polymers 13 (17) (2021) 2995.
[35] M.B. da Cruz, J.F. Marques, G.M. Peñarrieta-Juanito, M. Costa, J.C. Souza, R. S. Magini, G. Miranda, F.S. Silva, A. da Mata, J.M.M. Caramês, Hard and soft tissue cell behavior on polyetheretherketone, zirconia, and titanium implant materials, Int. J. Oral Maxillofac. Implants 34 (1) (2019) 39–46.
[36] M.B. da Cruz, J.F. Marques, G.M. Peñarrieta-Juanito, M. Costa, J.C.M. Souza, R. S. Magini, G. Miranda, F.S. Silva, J.M.M. Caramês, A. da Mata, Bioactive-enhanced polyetheretherketone dental implant materials: mechanical characterization and cellular responses, J. Oral Implantol. 47 (1) (2021) 9–17.
[37] S.M. Kurtz, J.N. Devine, PEEK biomaterials in trauma, orthopedic, and spinal implants, Biomaterials 28 (32) (2007) 4845–4869.
[38] A.A. Stratton-Powell, K.M. Pasko, C.L. Brockett, J.L. Tipper, The biologic response to Polyetheretherketone (PEEK) Wear particles in Total joint replacement: a systematic review, Clin. Orthop. Relat. Res. 474 (11) (2016) 2394–2404.
[39] F. Renò, V. Traina, S. Gatti, E. Battistella, M. Cannas, Functionalization of a poly(D, L)lactic acid surface with galactose to improve human keratinocyte behavior for artificial epidermis, Biotechnol. Bioeng. 100 (1) (2008) 195–202.
[40] T. Matsui, Y. Arima, N. Takemoto, H. Iwata, Cell patterning on polylactic acid through surface-tethered oligonucleotides, Acta Biomater. 13 (2015) 32–41.
[41] A. Saraswathibhatla, D. Indana, O. Chaudhuri, Cell-extracellular matrix mechanotransduction in 3D, Nat. Rev. Mol. Cell Biol. 24 (7) (2023) 495–516.
[42] P. Chieosilapatham, C. Kiatsurayanon, Y. Umehara, J.V. Trujillo-Paez, G. Peng, H. Yue, L.T.H. Nguyen, F. Niyonsaba, Keratinocytes: innate immune cells in atopic dermatitis, Clin. Exp. Immunol. 204 (3) (2021) 296–309.
[43] M. Piipponen, D. Li, N.X. Landén, The immune functions of keratinocytes in skin wound healing, Int. J. Mol. Sci. 21 (22) (2020).
[44] G. Mestrallet, N. Rouas-Freiss, J. LeMaoult, N.O. Fortunel, M.T. Martin, Skin immunity and tolerance: focus on epidermal keratinocytes expressing HLA-G, Front. Immunol. 12 (2021) 772516.
[45] M.D. Turner, B. Nedjai, T. Hurst, D.J. Pennington, Cytokines and chemokines: at the crossroads of cell signalling and inflammatory disease, Biochim. Biophys. Acta 1843 (11) (2014) 2563–2582.
[46] V. Karri, C. Lidén, N. Fyhrquist, J. Högberg, H.L. Karlsson, Impact of mono-culture vs. co-culture of keratinocytes and monocytes on cytokine responses induced by important skin sensitizers, J. Immunotoxicol. 18 (1) (2021) 74–84.
[47] I.O.o. Standardization, Biological evaluation of medical devices, Part 10: Tests for skin sensitization, 2021.
[48] M.D. Seo, T.J. Kang, C.H. Lee, A.Y. Lee, M. Noh, HaCaT keratinocytes and primary epidermal keratinocytes have different transcriptional profiles of cornified envelope-associated genes to T helper cell cytokines, Biomol. Ther. (Seoul) 20 (2) (2012) 171–176.
[49] A.R. Bowen, A.N. Hanks, S.M. Allen, A. Alexander, M.J. Diedrich, D. Grossman, Apoptosis regulators and responses in human melanocytic and keratinocytic cells, J. Invest. Dermatol. 120 (1) (2003) 48–55.